water

MDPI

Article

Water–Rock Interaction Processes in Groundwater and Flows in a Maar Lake in Central Mexico

Selene Olea-Olea [1,2,*], Raúl A. Silva-Aguilera [3], Javier Alcocer [2], Oscar Escolero [4], Eric Morales-Casique [4], Jose Roberto Florez-Peñaloza [3], Kevin Alexis Almora-Fonseca [5] and Luis A. Oseguera [2]

1 Dirección General de Asuntos del Personal, Universidad Nacional Autónoma de México, Posdoc Fellowship, Ciudad Universitaria, Ciudad de México 04510, Mexico
2 Grupo de Investigación en Limnología Tropical, FES Iztacala, Universidad Nacional Autónoma de México, Av. De los Barrios No. 1, Los Reyes Iztacala, Tlalnepantla 54090, Mexico; jalcocer@unam.mx (J.A.); loseguera.72@gmail.com (L.A.O.)
3 Posgrado en Ciencias del Mar y Limnología, Universidad Nacional Autónoma de México, Ciudad Universitaria, Ciudad de México 04510, Mexico; joserflorezp@hotmail.com (J.R.F.-P.)
4 Departamento de Dinámica Terrestre Superficial, Instituto de Geología, Universidad Nacional Autónoma de México, Ciudad Universitaria, Ciudad de México 04510, Mexico; ericmc@geologia.unam.mx (E.M.-C.)
5 Posgrado en Ciencias de la Tierra, Instituto de Geología, Universidad Nacional Autónoma de México, Ciudad Universitaria, Ciudad de México 04510, Mexico; kevin.almora96@gmail.com
* Correspondence: selene@geologia.unam.mx

Abstract: Tropical maar lakes are distinct ecosystems with unique ecological features. To comprehend, manage, and conserve these lakes, it is essential to understand their water sources, particularly groundwater, and the hydrogeochemical processes shaping their water chemistry. This research focuses on the maar lake Alchichica in central Mexico, known for harboring 18 new and endemic species and a ring of stromatolites. With groundwater discharge as the primary source, concerns arise over anthropic extraction impacts on water levels and stromatolite survival. Sampling six wells and one piezometer revealed major ion (Ca^{2+}, Mg^{2+}, K^{+}, Na^{+}, Cl^{-}, HCO_3^{-}, SO_4^{2-}) and trace element (Fe, Al^{3+}, SiO_2) concentrations. Geochemical evolution was explored through diagrams, geological sections, and inverse geochemical models using the PHREEQC code. Findings indicate groundwater evolving along controlled flow paths, and influencing chemical composition through water–rock interactions. The lake's unique conditions, resulting from the mixing of two flows, enable stromatolite formation. Water level reduction appears unrelated to evaporation at the sampled sites, suggesting a need for a broader study in a larger area. Analyzing the maar lake's hydrochemistry provides valuable insights into unique characteristics supporting high endemism in this ecosystem. This research enhances our understanding of groundwater's geochemical processes and hydrogeochemical evolution in maar lakes, with potential applications worldwide.

Keywords: maar lake; geochemical model; precipitation; dissolution; PHREEQC

Citation: Olea-Olea, S.; Silva-Aguilera, R.A.; Alcocer, J.; Escolero, O.; Morales-Casique, E.; Florez-Peñaloza, J.R.; Almora-Fonseca, K.A.; Oseguera, L.A. Water–Rock Interaction Processes in Groundwater and Flows in a Maar Lake in Central Mexico. *Water* **2024**, *16*, 715. https://doi.org/10.3390/w16050715

Academic Editor: Maurizio Barbieri

Received: 19 January 2024
Revised: 12 February 2024
Accepted: 24 February 2024
Published: 28 February 2024

1. Introduction

A maar lake is a water body formed by groundwater and/or precipitation filling an ancient volcanic depression [1]. A maar forms by underground phreatomagmatic explosions produced when hot magma encounters shallow groundwater, creating a violent steam explosion. The cavity is usually small, round, with low rims, and deep (i.e., up to 300 m). When filled with groundwater(most often) or rainwater, it constitutes a maar lake (volcanic type) [2]. Maar lakes are commonly found in young volcanic regions of the planet, like the Eifel district, Germany [3].

The lakes provide water for human activities and ecosystem services [4]. The research of tropical maar lakes around the world, including in Asia [5–8] and Africa [9–11], shows the importance of studying and understanding the functioning of these unique lakes.

The maar lake Alchichica in central Mexico stands out for its unique ecological characteristics and unparalleled high endemicity. To date, 18 new species have been described for Lake Alchichica, ranging from bacteria to amphibians and fish. Most of these are of restricted distribution; although they are endemic, most are considered micro-endemic because they only live in this lake. One of the internationally best-known species is the axolotl *Ambystoma taylori*, the only species in the world that lives in salt water. Another species of great relevance is the silverside fish *Poblana alchichica*, which is subject to a local fishery. Both species are listed as threatened and protected by law. However, the most crucial feature that has given the lake international recognition is the ring of stromatolites, living modern analogs of the first known life form on the planet [12,13].

Alchichica microbialites have been widely studied, both in terms of the species that form them and the ecological functions that they carry out. Both characteristics are closely linked with the recycling and transformation of the main elements of life, such as carbon, nitrogen, phosphorus, sulfur, and some trace metals. These elements circulate in biogeochemical cycles through the living (i.e., living beings) and non-living compartments (atmosphere, lithosphere, and hydrosphere), and are therefore related to productivity, the lake's biodiversity, and the quality of water, air, and sediments, since an excess of these elements results in pollution and eutrophication (excess nutrients) of aquatic bodies [12,13].

Combining the ground and surface water chemistries resulted in a unique chemical composition for Lake Alchichica waters, where groundwater is the major input because the precipitation in the study area is low [13]. The chemical interchange of both water masses and their mediation by microbial activity promotes the build-up of a ring of stromatolites (microbialites) parallel to the shoreline [13]. Also, the unique chemical composition of the Lake Alchichica waters is the most plausible reason to explain the incredibly high microendemicity in a relatively small and geologically young lake, which contrasts with the reduced species richness [12].

Lake Alchichica receives groundwater seeping out of the porous tephra of its associated volcanic edifice, and potentially experiences water loss to the underlying groundwater reservoir, meaning it essentially functions as a groundwater outcrop. Fluctuations in water levels are influenced by climatic changes and, possibly, groundwater extraction. A terrace surrounding the current lake shore, at the ancient littoral zone of Lake Alchichica, suggests a historically higher groundwater level. This elevated level corresponds to the water body responsible for the formation of the stromatolites encircling the lake today [14]. Although the maar lake is primarily fed by groundwater discharge, challenges such as intensive groundwater extraction [15] may impact the lake's water levels and hydrogeochemistry, and consequently, its biota (i.e., because the stromatolites need special hydrochemical conditions to form and thrive). When the water level decreases and the hydrochemistry changes, their persistence is affected.

Hydrochemical behavior in groundwater commonly exhibits spatial differences, and is primarily influenced by natural processes such as water–rock interactions [16]. In seeking to comprehend the hydrochemical behavior, geochemical models provide viable alternatives along a flow path. These models serve as simplified representations of reality. The approach of inverse geochemical modeling attempts to interpret the hydrochemical changes along a flow path [16]. The use of geochemical code PHREEQC [17] facilitates the performance of these geochemical models. Notably, the modeling of aqueous systems relies on the foundational assumption of chemical equilibrium among the dissolved species [18].

Numerous studies have explored aspects of Lake Alchichica, ranging from biodiversity [14,19–25] to limnology [26–30] and water chemistry [14,31–35]. However, none have comprehensively analyzed and quantified the water–rock interaction processes in the groundwater flow system that feeds the lake, or have considered if these processes can be related to the decrease of the lake level and the exposure of the stromatolites to air. The chemical composition of Lake Alchichica does not display seasonal variations [14,28,31,36], and so geochemical models were used to understand chemical behavior and evolution. Such models have been applied globally (e.g., [37–40]) and in Mexico (e.g., [41–45]) to

quantify dissolution, precipitation, or the evaporation process in groundwater, and identify changes in the water flow trajectories.

Therefore, this study represents the first attempt to comprehensively study and quantify water–rock interaction processes in groundwater flowing to and through the tropical Lake Alchichica. The aims of this research are to:

(i) Provide a comprehensive understanding of the geochemical evolution in the groundwater feeding Lake Alchichica.
(ii) Quantify the water–rock interaction processes in groundwater and the flow through this tropical maar lake.
(iii) Identify the primary reactions shaping the hydrochemistry of the groundwater.

The outcomes of this research will contribute significantly to our understanding of the chemistry of worldwide tropical maar lakes.

2. Study Area

Lake Alchichica is in the "Llanos de San Juan" sub-basin, and is part of the Serdán Oriental Basin (SOB) that extends to portions of the Puebla, Tlaxcala, and Veracruz states, central Mexico, covering a surface of 5250 km^2. The climate in the basin ranges from temperate arid to temperate semi-arid. The mean temperature is 13.9 °C, the precipitation is 392 mm and the evaporation is 1685.9 mm [46]. SOB is an endorheic basin with scarce surface runoff [47], and groundwater is therefore fundamental to the lake's water balance and chemistry [31]. Due to the endorheic characteristics of the basin, the primary water outflows manifest as surface evaporation from the bodies of water [47].

Since the early 1980s, many wells have been drilled in the vicinity of Lake Alchichica for groundwater exploitation. Approximately eighty percent of the extracted groundwater is allocated for irrigation, a proportion that has been on the rise, concomitant with the expansion of agricultural activities [48].

The main aquifer is in the basin's lowest part, and is formed by pyroclastic and lava materials with high hydraulic conductivity. Citlaltepetl-Cofre de Perote mountain range, which lies to the E, and La Malinche, to the S, are the main recharge areas [49]. The study area encompasses Lake Alchichica and groundwater flows to the lake from the SW and SE (Figure 1).

Lake Alchichica's surface exhibits a topographic gradient of 1 m with a SE to NW orientation, and is corroborated by groundwater flow nets [50–53], indicating that both groundwater inflows and outflows follow the same directional pattern. The flow nets of previous studies reveal a minimum of two inflow zones, one to the SE and another to the E, along with at least one outflow zone to the N [31].

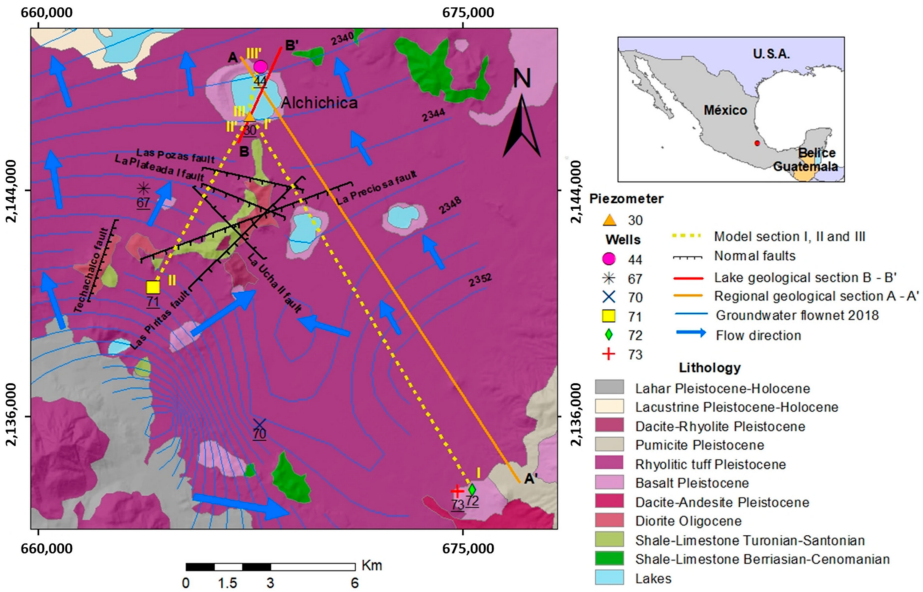

Figure 1. Study area, with sampling points, geology and faults. The geology and faults were taken from [54].

3. Geology

The SOB is a monogenetic volcanic field of quaternary age. The basin comprises dome complexes, scoria cones, tuff rings, and six maar lakes: Alchichica, Atexcac, La Preciosa, Quechulac, Aljojuca, and Tecuitlapa [55–57]. The basin is geologically configured by highly folded and faulted Cretaceous limestones and shales. The regional basement is overlaid by large pyroclastic deposits that originated in both large eruptions from adjacent volcanoes and local phreatomagmatic volcanoes. Some basin zones have a top layer of lacustrine deposits [55,58].

The volcanic and sedimentary units are: (i) Quaternary pumicite, lahar, basalt, dacite-ryolite, dacite-andesite, lacustrine and diorite, (ii) Paleogene, diorite and (iii) Cretaceous shale-limestone of Berriasian–Cenomanian and Turonian–Santonian origin. The structural features are six normal faults named: Las Pozas, La Plateada 1, La Preciosa, Las Piritas, La Uchala II, and Techachalco [54].

Mineralogy

The rocks in the study area are composed of rock-forming minerals of: (a) volcanic rocks, such as quartz, plagioclase, pyroxene, feldspar, albite, anorthite, calcite, and paragonite, with lithic fragments of obsidian. Additionally, ferromagnesian, as biotite and amphibole, is present, and so are (b) limestones with calcite, gypsum and anhydrite [49,55,58].

4. Methodology

4.1. Sampling, Data Analysis and Water Table

To understand the hydrogeochemistry of the groundwater that flows to Lake Alchichica, and to evaluate the impact of the water–rock interaction process on the lake's water level and biota, two groundwater sampling campaigns were carried out: the first one comprised 35 points (34 wells and 1 piezometer, February 2018, unpublished data), and the second one comprised seven points as one-time sampling (6 wells and 1 piezometer, November 2021, this study). In both sampling campaigns the physicochemical parameters of groundwater were measured using a multiparametric probe (HANNA HI9828). The sonde was calibrated before the sampling every day of the sensors of pH and electrical conductivity (EC), to measure pH, T (°C), EC (µS/cm) and total dissolved solids (TDS, ppm). Samples for major ion evaluation were taken in both campaigns. However, water–rock interaction processes could only be studied in volcanic rocks, with trace elements that formed silicate minerals (Fe, Al^{3+}, and SiO_2). For this reason, a second sampling campaign was carried out to sample trace elements at the 7 selected points where groundwater flows to and through Lake Alchichica. Sampling was carried out at the end of the rainy season.

We sampled 30 mL of water in polypropylene bottles, having previously filtered it through 0.45 µm nitrocellulose membranes to remove particles of water that could change the laboratory determination of cations (Ca^{2+}, Mg^{2+}, K^+, Na^+) and anions (Cl^-, HCO_3^-, SO_4^{2-}). Bottles were filled and sealed hermetically and kept at 4 °C until the analysis. Samples were analyzed by liquid chromatography at the Laboratory of Chromatography in the Institute of Geology, National Autonomous University of Mexico. For the trace element quantification, a 30 mL sample was taken in polypropylene bottles at each point, filtering the volume through a 0.45 µm nitrocellulose membrane and acidifying the sample with HNO_3 at pH ~2. Trace elements (Fe, Al^{3+}, and SiO_2) samples in water were prepared according to the US EPA 200.7 method [59]. Analyses were developed with a Perkin Elmer (Waltham, MA, USA) Optima 8300 device with a seaspray nebulizer and a baffle chamber (double pass), and in accordance with the US EPA 6010D method [60], using inductively coupled plasma—optical emission spectrometry in the Atomic Spectroscopy Laboratory of the Institute of Geology, National Autonomous University of Mexico. The accuracy of ion

laboratory analyses was tested using the charge balance error (CBE) equation (Equation (1)), with values considered against an acceptable limit of ±5% [16,53,54,61].

$$\text{CBE\%} = \frac{(\sum \text{Cations})\text{mEq/L} - (\sum \text{Anions})\text{mEq/L}}{(\sum \text{Cations})\text{meq/L} + (\sum \text{Anions})\text{meq/L}} \times 100 \quad (1)$$

In February 2018, water levels were measured using a water level sensor SOLINST with an accuracy of millimeters to determine the water table configuration in the study area. We employed spatial interpolation of water table elevations through the ordinary Kriging method [62,63]. The values used for the interpolation of flow network are located in the same aquifer, at depths of approximately 70 and 120 m.

4.2. Hydrochemical Diagrams

We use the trilinear diagram of Piper [64] to help illustrate variations in groundwater chemistry throughout the study area. Gibbs plot is used to determine the dominant hydrogeochemical processes (precipitation, water–rock interaction, and evaporation) that control groundwater chemistry [65,66]. The use of this diagram in groundwater facilitates the delineation and characterization of the intricate interaction between water and the surrounding rock formations [66].

The stability diagrams were also used to evaluate the equilibrium trends between silicate minerals and natural water on the basis of thermodynamic calculations. These diagrams were developed for different silicate mineral phases at 25 °C and 1 atm, using the activities of dissolved species at thermodynamic equilibrium in a given set of conditions (T, pH, redox potential, total content of each metal in solution) determined with PHREEQC code [17]. The dynamic equilibrium between solutions and coexisting solid phases is shown in the stability diagrams, and they are used to interpret the geochemical behavior of natural water in terms of water–rock interactions [67]. These diagrams were used to understand predominant trends in silicate hydrolysis, where the mineral stability of phases depends on the physicochemical conditions of the system.

4.3. Saturation Index

The resulting models encompass all potential reactions to elucidate variations in the composition of the flow path. However, a pragmatic approach was adopted, and the most plausible model was selected for each corresponding section. Groundwater, through its interaction with surrounding rocks, undergoes increased mineralization as a result of the dissolution and precipitation of minerals. This phenomenon can be quantified using the Saturation Index (SI) Equation (2):

$$\text{SI} = \log \frac{IAP}{Ks} \quad (2)$$

Here, *IAP* represents the ion activity product of the solution, and *Ks* denotes the solubility product of the mineral.

Equilibrium, indicating saturation concerning the specific mineral in question, is achieved when SI = 0. A negative SI (<0) implies subsaturation, leading to mineral dissolution, while a positive SI (>0) indicates supersaturation, necessitating mineral precipitation [16,61].

The saturation indices of albite, calcite, dolomite, gypsum, halite and kaolinite of the seven samples were determined with PHREEQC [17], version 3.0.

4.4. Geochemical Models

While the chemistry in the groundwater sites of the surrounding area of Lake Alchichica presents high and low ionic concentrations, they do not suggest a clear evolution of groundwater. To understand the processes that caused this, it is recommended to study the geochemical evolution in a groundwater flow line, where water has an initial and final composition. Addi-

tionally, as mentioned, the chemical composition of water in Lake Alchichica does not present seasonal variations, which suggests that groundwater has the same behavior. Nevertheless, chemical variations cannot be associated with seasonality. For a comprehensive understanding of the chemical reactions governing the geochemical composition of two groundwater sites, we opted for the application of geochemical models. These models, which provide simplified representations of reality, enable us to elucidate the intricate water–rock interaction processes influencing ion concentrations in groundwater. To assess the equilibrium state of groundwater in selected mineral phases, we specifically chose the PHREEQC code [17], version 3.0, along with the phreeqc.dat database and complementary hydrogeochemical phases (Table 1). The use of PHREEQC and its robust database establish a suitable tool for evaluating water-rock interaction processes.

Table 1. Mineral phases and their solution reactions used in the inverse modeling process (References: 1 [17]; 2 [68]; 3 [69]; 4 [70].

Phase	Reaction	Ref.
CO_2 (g)	$CO_2(g) = CO_2(a)$	1
H_2O (g)	$H_2O(g) = H_2O(a)$	1
Albite	$NaAlSi_3O_8 + 8H_2O = Na^+ + Al(OH)_4^- + 3H_4SiO_4$	1
Calcite	$CaCO_3 = CO_3^{2-} + Ca^{2+}$	1
Dolomite	$CaMg(CO_3)^2 = Ca^{2+} + Mg^{2+} + 2CO_3^{2-}$	1
Gypsum	$CaSO_4{\cdot}2H_2O = Ca^{2+} + SO_4^{2-} + 2H_2O$	1
Halite	$NaCl = Na^+ + Cl^-$	1
SiO_2 (aq)	$SiO_2 + 2H_2O = H_4SiO_4$	1
Kaolinite	$Al_2Si_2O_5(OH)_4 + 6H^+ = H_2O + 2H_4SiO_4 + 2Al^{3+}$	1
Biotite	$KMg_3AlSi_3O_{10}(OH)_2 + 6H^+ + 4H_2O = K^+ + 3Mg^{2+} + Al(OH)_4^- + 3H_4SiO^4$	1
Plagioclase	$Na_{0.62}Ca_{0.38}Al_{1.38}Si_{2.62}O_8 + 5.52H^+ + 2.48H_2O = 0.62Na^+ + 0.38Ca^{2+} + 1.38Al^{3+} + 2.62H_4SiO_4$	1
Glass	$Si_{1.0}Al_{0.35}O_2(OH)_{1.05} + 1.05H^+ + 0.95H_2O = 0.35Al^{3+} + H_4SiO_4$	2
Piroxene	$CaFeSi_2O_6 + 4H^+ + 2H_2O = Ca^{+2} + Fe^{+2} + 2H_4SiO_4$	3
Amphibole	$Ca_2Mg_5Si_8O_{22}(OH)_2 + 14CO_2 + 22H_2O = 2Ca^{2+} + 5Mg^{2+} + 14HCO_3^- + 8H_4SiO_4$	4

Inverse modeling was employed to identify hydrogeochemical processes that explain the hydrochemical evolution of groundwater [71–73]. This mass-balance approach uses two water samples from wells or piezometers, representing the initial and final chemical compositions of water along a flow path, to calculate the moles of minerals and gases that may enter or exit the solution, accounting for the differences in composition [74]. The inverse modeling application is based on some assumptions: (1) the final water must be evolved from the initial water, (2) hydrodynamic dispersion and diffusion have a negligible effect on groundwater chemistry, (3) a chemical steady state condition prevailed in the groundwater system during the time considered, (4) the mineral phases used in the mass balance calculation currently exist or were previously present in the host rock formations [75].

The geochemical inverse modeling was used to better understand geochemical processes in groundwater to and through Lake Alchichica. Three model sections were used to develop the inverse geochemical models.

The number of inverse models obtained was reduced to the minimum phase models that satisfy the restrictions within the specified uncertainty limits. The minimum models imply that no model with any proper subset of phases and solutions could be found by minimizing the number of calculations produced by the models that contain the essential geochemical reactions [17]. Hence, the minimum models for each section were presented in results.

Four samples were selected to apply inverse geochemical models; the selection criterion was the regional flow direction towards the lake and leading to piezometer 30; samples 71 and 72 were selected to represent chemical composition at the start of the groundwater flow path, close to recharge areas. Groundwater then flows into the lake and flows back into the aquifer along the northern shore of the lake (Figure 1). Well 44 was selected as representative of this groundwater flow with an important proportion of water from the lake, because the lake bottom is about 18 m deeper than well 44 (water level in Lake Alchichica is about 2326 m.a.s.l. and the lake is 62 m deep; Well 44 is located at an elevation

of 2352 m.a.s.l. and has a depth of 70 m).In according with mineralogy data from the study area we use different reactive phases described in Table 1. According to previous researchers, it was assumed that the groundwater samples do not present seasonal variations in the hydrochemistry and represent the evolution along the flow path [14,31–34,76].

The resulting models encompass all potential reactions to elucidate variations in the composition of the flow path. However, a pragmatic approach was adopted, and the most plausible model was selected for each corresponding section.

4.4.1. Section I-I′

Section I-I′ (Figure 1) is oriented SE-NW and cuts across the La Preciosa and Las Piritas faults. There is a distance of 15 km, approximately, between Well 72 (initial composition, 120 m deep) and piezometer 30 (final composition, 2.95 m deep). The mineral phases used in section I-I′ were CO_2(g), H_2O(g), calcite, dolomite, gypsum, biotite, halite, SiO_2(aq), kaolinite, pyroxene, glass and albite, with an accepted uncertainty in the model of 0.08. The conceptual model for this section explains that rainwater infiltrates the subsoil in the unsaturated zone and begins to dissolve CO_2 (which mainly originates in the edaphic zone, probably by organism respiration and organic matter decomposition [61]), and then flows in the direction of Lake Alchichica and interacts with the rocks and faults. This model section is parallel to the regional geological section A–A′ (Figure 2a). Hence, we used the former to indicate the flow direction and well and piezometer location.

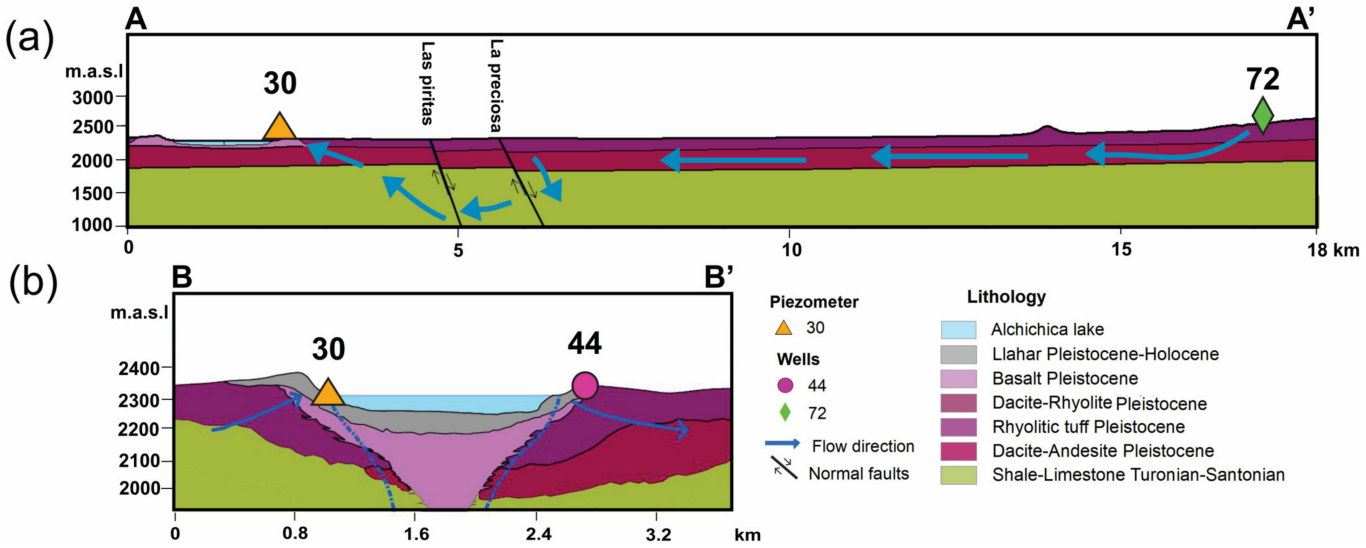

Figure 2. Geological sections of Lake Alchichica: (**a**) regional and (**b**) local sections.

4.4.2. Section II-II′

Section II-II′ (Figure 1) is oriented SE-NW, and cuts through the faults of Las Pozas, La Plateada I and La Ucha II [54]. Well 71 (initial composition, depth of well is unknown) and piezometer 30 (final composition, 2.95 m deep) are separated by 7 km, approximately. The mineral phases used in section II-II′ were CO_2(g), H_2O(g), calcite, dolomite, gypsum, biotite, halite, SiO_2(aq), kaolinite, plagioclase, and albite, with an accepted uncertainty in the model of 0.08. While the conceptual model is the same as in Section I–I′, no geological section is presented in this model section.

4.4.3. Section III-III′

Section III-III′ (Figure 1) is oriented SE-NW and passes through Lake Alchichica. The piezometer 30 (initial composition, 3 m deep) to Well 44 (final composition, 70 m deep) are separated by 2 km approximately. The mineral phases used in section III-III′ were CO_2(g), H_2O(g), calcite, gypsum, biotite, halite, SiO_2 (aq), kaolinite, pyroxene, amphibole and albite, with an accepted uncertainty in the model of 0.07. The conceptual model for

this section explains that groundwater that reaches the Lake Alchichica has an evolved chemical composition (a product of the previous interaction with the rocks in the flow path); it crosses the lake, where it interacts with the lake water to produce a mixture, and then flows through the lake before finally arriving to the groundwater again in Well 44. This section is almost parallel to the lake's geological section B–B′ (Figure 2a). Hence, we used it to indicate the flow direction in the piezometer and well.

5. Results

5.1. General Groundwater Context

This sub-section provides a summary of the results: (1) water table direction is mainly from SE to NE (Figure 1). (2) Ion concentrations and the physiochemical parameters of the sites present different values (Table 2), and do not show a clear tendency to increase or decrease. (3) In the Piper diagram, all the samples are placed in magnesium-sulphate waters, with the exception of the piezometer 30, which is in the limits of sodium-chloride waters (Figure 3). (4) In the Gibbs diagram (Figure 4), all the samples are in the rock dominance, and are positioned in the direction of silicates weathering. (5) Almost all the samples are in the kaolinite stability field (Figure 5), except for Mg^{2+} in Well 70 (Figure 5b).

Table 2. Ranges of physicochemical parameters of samples. (m E = meters East, m N = meters North, LOD = limit of detection).

Name	Units	30	44	67	70	71	72	73
Depth	m	3	70	100	-	-	120	120
m E	m	667,464	667,843	663,706	667,801	664,057	675,331	674,813
m N	m	2,146,637	2,148,401	2,144,092	2,135,736	2,140,589	2,133,441	2,133,403
pH	pH units	7.2	7	7.5	8.3	7.1	8	7.9
T	°C	18.5	21.6	20	19.2	25.1	15.8	14,6
EC	µS/cm	1479	1950	1793	526	2420	139	126.7
TDS	ppm	740	975	894	263	1220	69.2	63.7
Ca^{2+}	mg/L	25.3	4	70.6	44.1	118.8	12.3	11.1
Mg^{2+}	mg/L	70	278.2	124.3	25.6	139.3	5.9	5.6
Na^{+}	mg/L	147.7	183.3	122.2	33.3	137.2	10.1	9.9
K^{+}	mg/L	8.5	15.1	10.7	3.9	12.9	3.5	3.7
Cl^{-}	mg/L	104.3	174.1	210.6	33.6	311.6	4.1	3.5
SO_4^{2-}	mg/L	56.1	12	92.9	12.2	66.9	3.8	4.4
HCO_3^{-}	mg/L	702.5	1738.0	811.5	266.9	1052.5	76.6	72.1
Al^{3+}	mg/L	1.4	0.03	<LOD	<LOD	<LOD	0.02	<LOD
SiO_2	mg/L	70.6	75	82.3	51.2	86	46.8	46.5
Fe	mg/L	3.6	1.9	1.7	<LOD	3.6	<LOD	<LOD

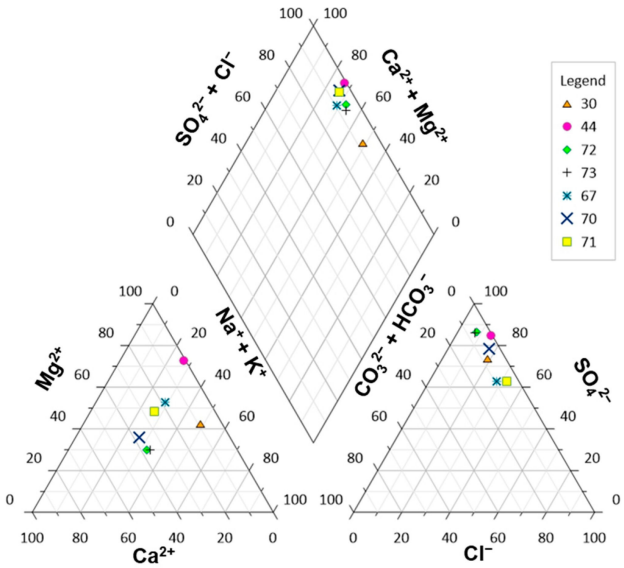

Figure 3. Piper diagrams of piezometer and wells.

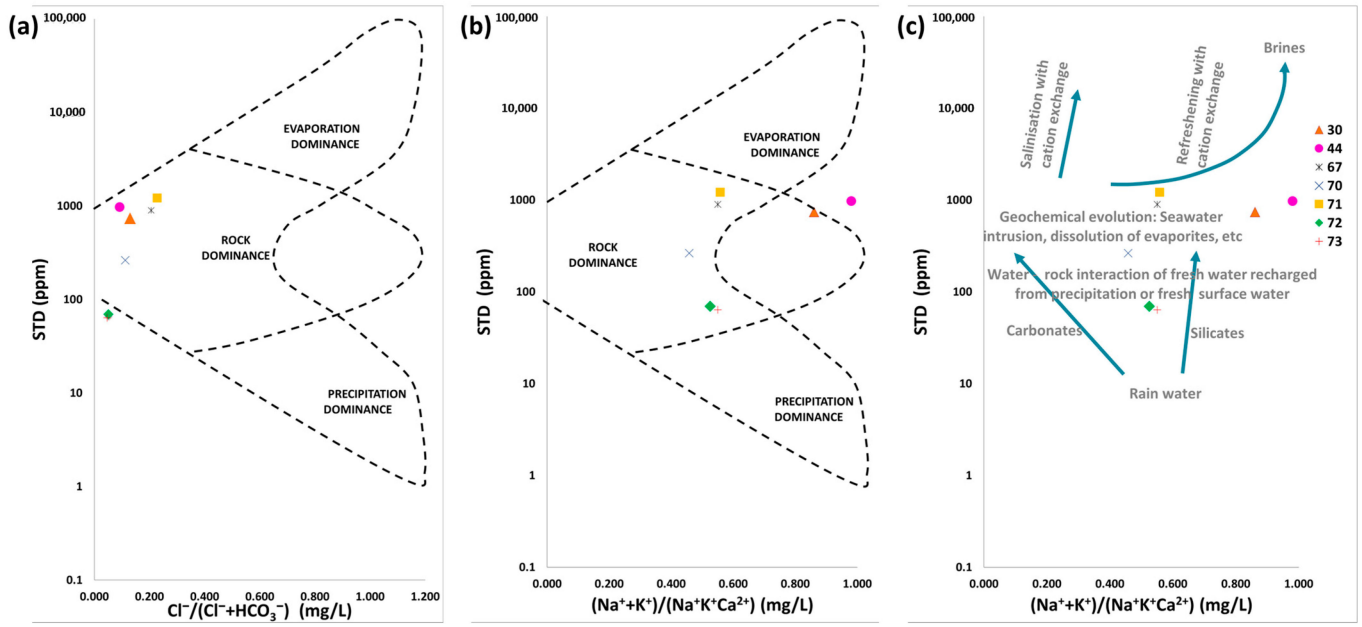

Figure 4. Gibbs diagrams (**a**) anions, (**b**) cations, (**c**) modified Gibbs diagram, according to [66].

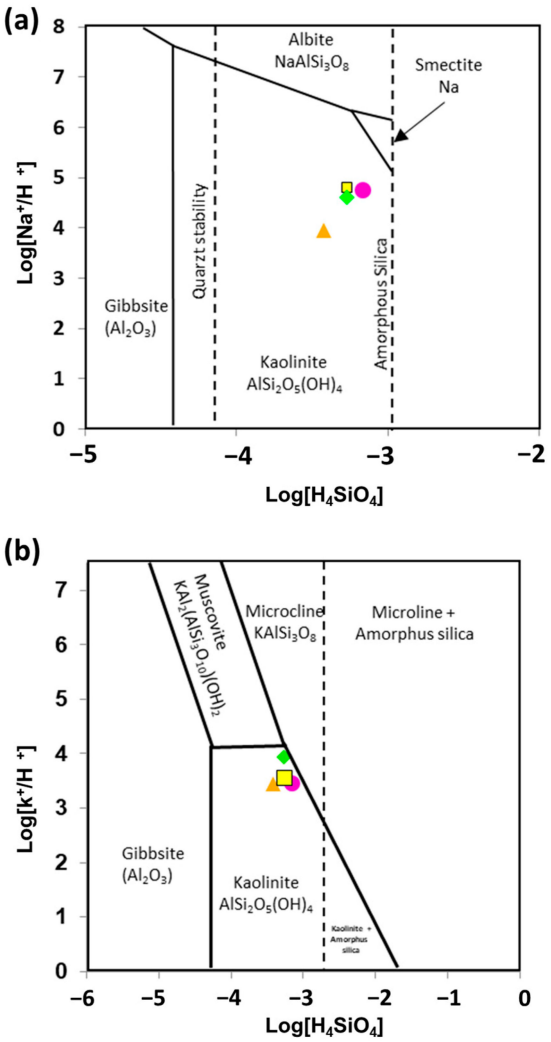

Figure 5. *Cont.*

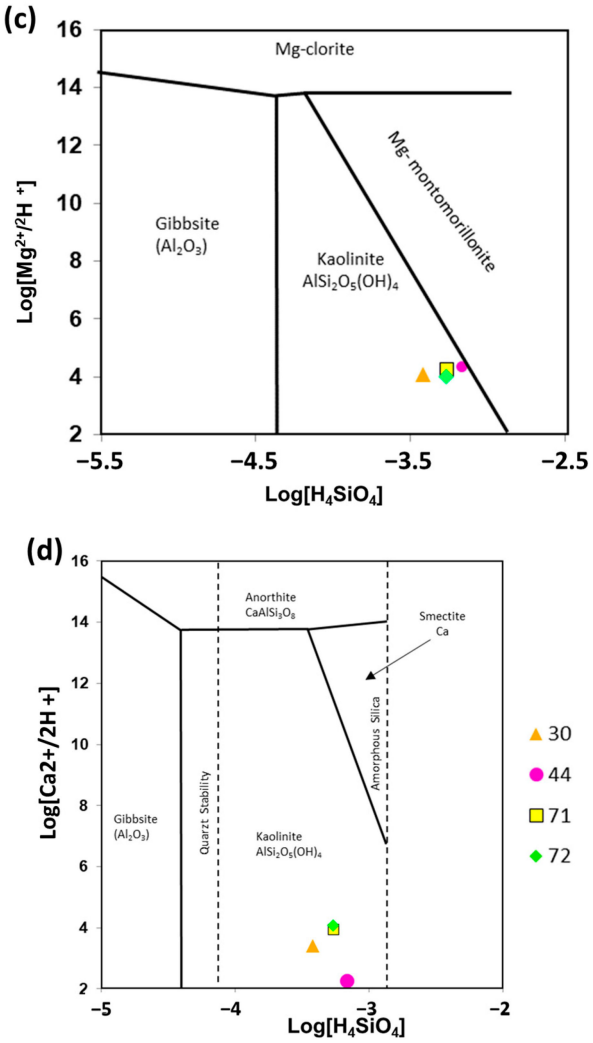

Figure 5. Stability diagrams of (**a**) Na_2O, (**b**) K_2O (**c**) MgO (**d**) CaO-H_2O-SiO_2 systems at 25 °C and 1 atm.

While no clear tendency in the data is shown in the results, the geochemical models help us to understand the processes that produce these geochemical compositions.

Ion concentrations, physicochemical parameters, location, and the depth of the samples are shown in Table 2.

The SI values reveal the undersaturation of halite and gypsum and the oversaturation of Kaolinite in all samples; the albite, calcite, and dolomite values do not present a preferent behavior for all the samples (Figure 6).

5.2. Mass Transfer Models

Inverse geochemical modeling led to three models for section I–I′, and two for sections II–II′ and III–III′ (Table 3). The reported models propose possible reactions in order to explain the geochemical composition of two groundwater sites, and it is necessary to select the more feasible model. In all selected models, precipitation of calcite, SiO_2(aq) and kaolinite are present. Dissolution of gypsum occurs in the first two sections, but not in section III–III′. In addition, CO_2(g), albite, dolomite, halite, biotite, glass, plagioclase, and amphibole are all in dissolution, except in Model II–II′, in which dolomite and halite precipitate'. Additionally, the H_2O is in dissolution and precipitation.

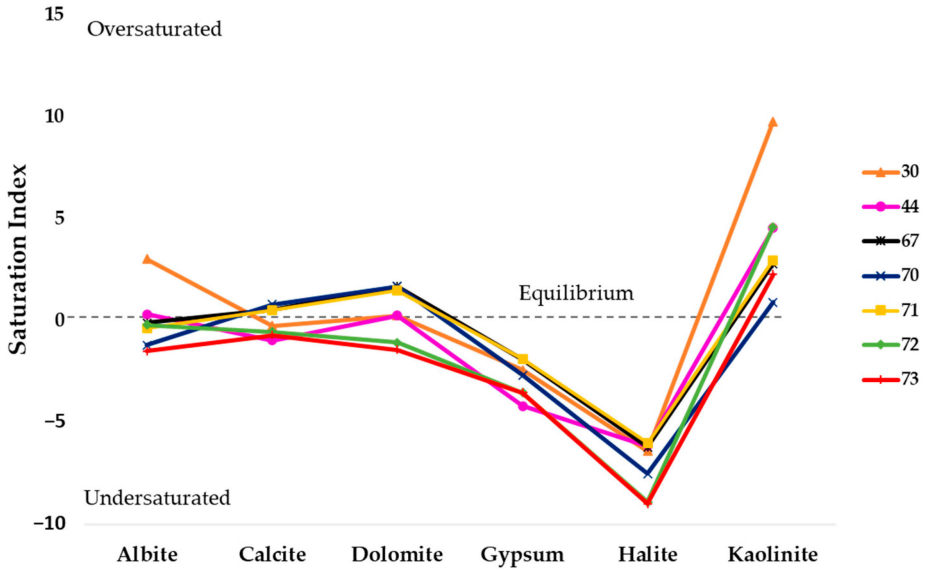

Figure 6. Saturation index plot of the sampling points.

Table 3. Summary of mass transfers for selected inverse geochemical models. Phases and thermodynamic data were taken from PHREEQC and accompanying databases [77] and Table 1. Note: Values are in moles per kilogram H_2O: positive values indicate dissolution, and negative values indicate precipitation. Dashes indicate the phase is not present in the model.

Phase	Section I-I′			Section II-II′		Section III-III′		Chemical Formula
Samples	**72–30**			**71–30**		**30–44**		
	Model 1	Model 2	Model 3	Model 1	Model 2	Model 1	Model 2	
CO_2(g)	9.37×10^{-3}	7.85×10^{-3}	1.04×10^{-2}	5.06×10^{-3}		2.48×10^{-2}	3.56×10^{-2}	CO_2
H_2O(g)		-7.93×10^{1}	5.55×10^{1}	1.59×10^{1}	1.28×10^{1}		4.36×10^{1}	H_2O
Albite	3.78×10^{-3}	3.33×10^{-3}	4.09×10^{-3}		5.27×10^{-3}		2.19×10^{-3}	$NaAlSi_3O_8$
Calcite	-2.67×10^{-3}	-3.08×10^{-3}	-2.38×10^{-3}	-3.39×10^{-3}		-3.28×10^{-3}	-3.99×10^{-3}	$CaCO_3$
Dolomite	2.47×10^{-3}	2.53×10^{-3}	2.43×10^{-3}	-1.41×10^{-3}	-1.77×10^{-3}			$CaMg(CO_3)_2$
Gypsum	5.45×10^{-4}	4.89×10^{-4}	5.85×10^{-4}			-4.48×10^{-4}		$CaSO_4{:}2H_2O$
Halite	2.68×10^{-3}	2.52×10^{-3}	2.80×10^{-3}	-2.84×10^{-3}	-3.30×10^{-3}	1.67×10^{-3}	4.32×10^{-3}	NaCl
SiO_2(a)	-7.46×10^{-3}	-7.43×10^{-3}	-7.48×10^{-3}	-1.03×10^{-2}	-1.05×10^{-2}	-1.28×10^{-2}	-1.99×10^{-2}	SiO_2
Kaolinite	-1.93×10^{-3}	-1.64×10^{-3}	-2.13×10^{-3}	-5.73×10^{-3}	-2.61×10^{-3}	-1.11×10^{-4}	-1.27×10^{-3}	$Al_2Si_2O_5(OH)_4$
Biotite	1.28×10^{-4}		2.17×10^{-4}			1.69×10^{-4}	3.40×10^{-4}	$KMg_3AlSi_3O_{10}(OH)_2$
Glass								$Si_{1.0}Al_{0.35}O_2(OH)_{1.05}$
Plagioclase				8.35×10^{-3}				$Na_{0.62}Ca_{0.38}Al_{1.38}Si_{2.62}O$
Amphibole						1.58×10^{-3}	1.98×10^{-3}	$Ca_2Mg_5Si_8O_{22}(OH)_2$

6. Discussion

6.1. General Groundwater Process

The Piper diagram (Figure 3) suggests that the piezometer located in the entrance area to Lake Alchichica has a different composition to the wells; these are congruent with the drilling depth because the wells are deeper to the piezometer; although the piezometer (30) displays a more evolved water, this is probably because it receives two different flows. The adapted Gibbs diagram in cations (Figure 4c) associates the water–rock interaction with silicate rocks, suggesting the geochemical evolution of groundwater can be explained in this way. Samples 71, 30, and 44 are close to evaporation (Figure 4), which would show the possible influence of evaporation on the decrease in groundwater table levels.

To better understand the evolution processes, stability diagrams confirm the dissolution of silicates (Figure 5), which is similar to the Gibbs diagram (Figure 4c). Almost all the samples are plotted in the kaolinite stability field (Figure 5), except one sample (Figure 5b), and, it can therefore be inferred that the chemistry of the groundwater system favors kaolinite formation, with one exception. This means that infiltrating water enriched with soil CO_2 reacts with silicate minerals from the host rocks (concretely albite, plagioclase,

biotite, and amphibole) leaches out Na^+, K^+, Mg^{2+}, and HCO_3^- and converts in kaolinite and silica.

6.2. Mass Transfer Model I–I′

The three minimum models that suggested the geochemical reactions that might produce the groundwater composition observed at piezometer 30 (in the lakeside) are shown in Table 2. The ion concentrations between the two sites (72 to 30) and the Gibbs diagram (Figure 4) suggest that water–rock interaction in silicate rocks increases the concentrations of the different ions and is the dominant process; Model 2 is not therefore considered accurate because it proposes that evaporative concentration is the dominant process. Models 1 and 3 represent the most plausible processes, which are dissolution of CO_2(g), albite, dolomite, gypsum, halite, and biotite with precipitation of calcite, SiO_2(aq) and kaolinite. The geological section A–A′ (Figure 2a) suggests that groundwater flowing through volcanic rocks reaches the underlying carbonate rocks through faults (La Preciosa and the Piritas) and then flows back to the same volcanic rocks before reaching the lake. Taking into account the water chemical evolution from SE to NW, the geological section A–A′ (Figure 2a) and the mineralogy [49,55,58] of the study area, it can be assumed that Model 3 would be the most plausible representation of water–rock interaction processes, and this is because it considers the dissolution in H_2O to be a process that favors the dissolution of minerals.

6.3. Mass Transfer Model II–II′

Two minimum models suggested the geochemical reactions that produced the groundwater composition in the SW to the piezometer in the lakeside. The ion concentrations between the two sites (71 to 30) decrease (Table 2), and the Gibbs diagram (Figure 4) suggests a rock dominance in silicate rocks. The models propose precipitation of calcite, dolomite, halite, SiO_2(aq), and kaolinite, with the exception of the calcite (Model 2); and dissolution (CO_2(g), H_2O, and plagioclase (Model 1); and H_2O and albite (Model 2). The location of the model section in the geologic map (Figure 1) suggested that groundwater flows through faults (La Ucha II, La Plateada I, and Las Pozas) from volcanic to carbonate rocks in deep water, and then enters shallow water again, flowing in volcanic rocks. Considering the water chemical evolution from SW to NE, and the ionic concentration that decreases mainly in Ca^{2+}, Mg^{2+}, HCO_3^-, and Cl^-, it can be assumed that Model 1 would be the more plausible model that represents water–rock interaction processes, and this is because it reproduced the decrease of ion concentrations caused by precipitation of more minerals to a greater extent than Model 2.

6.4. Mass Transfer Model III–III′

The minimum models and the geochemical reactions that might produce the groundwater composition through Lake Alchichica are shown in Table 2. The Piper diagram (Figure 3) suggested that the input piezometer (30) refers to more evolved water than the well of output (44). However, the Gibbs diagram states both sampled sites are influenced by rock interaction with silicate rocks (Figure 4). In addition, HCO_3^- concentration in this well (1738 mg/L) is the highest of the sampled sites, reflecting an evolved flow. This is consistent with the representation of groundwater discharging to Lake Alchichica, and Well 44 is representative of lake water flowing into the groundwater table (Figure 2b). The water–rock interaction processes suggested by the models are precipitation of calcite, gypsum, SiO_2(aq), and kaolinite; precipitation of gypsum does not occur in Model 2. At the same time, the minerals in dissolution in Model 1 are CO_2(g), halite, biotite, and amphibole, whereas in Model 2 they are CO_2(g), H_2O, albite, halite, biotite, and amphibole. Considering the waters' chemical evolution, the ionic concentration, the geological section in the lake B-B′ (Figure 2b), and the high increase of HCO_3^-, it can be assumed that Model 2 would be the more plausible representation of the water–rock interaction processes, and this is because it presents minerals as albite, amphibole, and kaolinite, which are a source of HCO_3^-.

6.5. Processes Controlling Groundwater Chemistry

The groundwater and hydrochemistry in the Lake Alchichica study area are controlled by the dissolution and precipitation of rock-formed minerals described in [49,55,58]. SI validates that the samples are undersaturated with halite and gypsum, while being oversaturated with kaolinite. The primary process identified and presented the following relations:

(a) calcite precipitation (Equation (3)) [78] is a product of the dissolution of primary silicates, as biotite, amphibole and pyroxene, from rocks in the study area, which produces Ca^{2+} in the solution,
(b) the dolomite dissolution originated increases of Ca^{2+} and Mg^{2+} (Equation (4)) [79] and, consequently, calcite precipitation, as mentioned previously,
(c) gypsum dissolution (Equation (5)) [80] and precipitation (Equation (6)) [81] could be related to Ca^{2+} increase in the groundwater, from primary silicates and $SO_4{}^{2-}$ from carbonate rocks,
(d) plagioclase dissolution gives Ca^{2+} and Na^{+} to water (Equation (7)) [82],
(e) albite dissolution causes kaolinite precipitation (Equation (8)) [83] is related to the increase of silica (Table 2),
(f) albite dissolution provokes increases of $HCO_3{}^{-}$ (Equation (9)) [84], which is linked to weak carbonic acid reacting with carbonate or silicate minerals to form $HCO_3{}^{-}$ ions (Equation (10)) [85],
(g) biotite dissolution produces increases of Mg^{2+} and K^{+} (Equation (11)) [86], and
(h) amphibole dissolution causes increases of Mg^{2+} and Ca^{2+} (Equation (12)) [87,88].

$$2HCO_3{}^{-} + Ca^{2+} \rightarrow CaCO_3\ (\text{calcite}) + H_2O \quad (3)$$

$$CaMg(CO_3)_2\ (\text{dolomite}) + 2H_2CO_3 \rightarrow Ca^{2+} + Mg^{2+} + 4HCO_3 \quad (4)$$

$$CaSO_4{\cdot}2H_2O\ (\text{gypsum}) \leftrightarrow Ca^{2+} + SO_4{}^{2-} + 2H_2O \quad (5)$$

$$Ca^{2+}(aq) + SO_4(aq) + 2H_2O = CaSO_4{\cdot}2H_2O(s)\ (\text{gypsum}) \quad (6)$$

$$10(Na_{0.8}Ca_{0.2})Al_{1.3}Si_{2.7}O_8\ (\text{plagioclase}) + 16H^{+} + 34H_2O \rightarrow 6Al_2Si_2O_5(OH)_4 + 15H_4SiO_4 + 2Ca_{2+} + 8Na_{+} + Al_{3+} \quad (7)$$

$$2NaAlSi_3O_8\ (\text{albite}) + 11H_2O \leftrightarrow Al_2Si_2O_5(OH)_4\ (\text{kaolinite}) + 2Na^{+} + 2HCO_3H_4SiO_4 \quad (8)$$

$$2NaAlSi_3O_8\ (\text{albite}) + 2CO_2 + 3H_2O \rightarrow Al_2Si_2O_5(OH)_4\ (\text{kaolinite}) + 2Na^{+} + 2HCO_3{}^{-} + 4SiO_2 \quad (9)$$

$$H_2CO_3\ (\text{carbonic acid}) + CaCO_3\ (\text{calcite}) \leftrightarrow Ca^{2+} + 2HCO_3{}^{-} \quad (10)$$

$$Si_3AlMgFe_2O_{10}(OH)_2K\ (\text{biotite}) + 10H^{+} = Al^{3+} + Mg^{2+} + 2Fe^{2+} + K^{+} + 3H_4SiO_4 \quad (11)$$

$$Na_{0.5}Ca_2(Fe_{1.3}Mg_{2.6}Al_{1.1})\ (Al_{1.6}Si_{6.4})O_2\ (\text{amphibole}) + 15H^{+} + H_2O \rightarrow 0.5Na + 2Ca^{2+} + 2.6Mg^{2+} + 1.3Fe^{2+} + 2.7Al(OH)_2{}^{+} + 6.4H_4SiO_4(aq) \quad (12)$$

To summarise, the igneous and carbonate rocks interact with groundwater through dissolution and precipitation. Consequently, the water–rock interaction processes in the study area represent an equilibrium system in which minerals are dissolved by hydrolysis and precipitated when the solution is saturated. The presence of Ca^{2+} in water is thought to be from the weathering of carbonates (calcite, dolomite and gypsum) and silicate minerals (plagioclase) [36,80,82], in contrast to the Mg^{2+} contents, which come from the weathering of silicate (biotite, amphibole) and carbonate (dolomite) minerals [44,45,85,89]. Furthermore, the Na^{+} origin could be related to weathering of plagioclase, albite and amphibole [82–84,87], and weathering of andesite rocks may deliver Na^{+} to water [44,45,90]. At the same time, the K^{+} contents could be related to biotite weathering [44,45,86,89]. Moreover, the Cl^{-} concentrations can be related to the weathering of hydrosilicate minerals (biotite, amphibole, and phyllosilicates) [45,91–93]. Finally, the high values of $HCO_3{}^{-}$ could be related to the weathering of carbonate (calcite and dolomite) and silicate (albite, amphibole and kaolinite) minerals [44,45,78,79,83,84].

Seasonal variations in the hydrochemistry of groundwater were discarded because several previous studies reported similar ion concentrations in the water column of Lake Alchichica [14,31–34,76]. The previous discussion explains that the geochemistry processes originated in the groundwater, and proposes points that will help observers to understand why the groundwater in the input of Lake Alchichica has these values. The presence of two flows with different water–rock interaction processes is the most relevant.

While the water–rock interaction processes identified in this study yield crucial insights into the groundwater evolution and behavior of Lake Alchichica, they do not offer an explanation for the observed decrease in Lake Alchichica's water level. Evaporation at the sample sites is deemed insignificant for groundwater, eliminating it as a substantial factor contributing to the observed decline. We recommend expanding this investigation across the entire SOB to encompass all maar lakes and their respective water–rock interaction processes. Such an extension would provide comprehensive information essential for understanding and addressing the broader issue of water level decrease in these maar lakes.

6.6. Limitations and Further Research Opportunities

The outcomes of geochemical modeling exhibit a pronounced dependence on the choice of mineral phases, constraints, and conceptual frameworks. Mass-balance models, while informative, lack a singular solution, as alternative models and outcomes may emerge based on distinct assumptions and constraints applied during the inverse modeling process.

Acknowledging that the resultant models represent one plausible scenario among a spectrum of potential processes governing water–rock interactions is crucial. We suggest using stable isotopes (O-18 and H-2) for a more robust model to evaluate the isotopic fractionation. The use of these isotopes gives information about the physical processes that control the water behavior (e.g., the relation of precipitation, evaporation, or recharge), which permits understanding of the relation of sampling sites with recharge or flow ways. Additionally, the radioactive isotopes (H-3 and C-14) allow the identification of the recharge age and give information on the residence time. Their combined use gives tools for a robust model with information that includes the recharge, discharge, and residence time.

In the study area, the presence of agricultural activities that have been reported since the 1980′s suggested the possible influence of fertilizer and herbicide in groundwater, but no studies have yet confirmed this. The geochemical model cannot evaluate these processes, so it is necessary to develop new studies.

7. Conclusions

The key findings of this study can be summarized as follows: (a) Groundwater flows towards Lake Alchichica in two directions: SE to NW and SW–NE. (b) The magnesic-sulfate type predominates in all wells, while the piezometer exhibits sodium–chloride waters at its limit. (c) Silicate weathering dominates rock composition. (d) Well 44, situated on the opposite side of Lake Alchichica, displays a more evolved concentration of HCO_3^-. (e) Faults in the study area suggest additional pathways of groundwater flow. (f) Groundwater chemical composition reflects the precipitation and dissolution processes of carbonate and silicate minerals. (g) The chemical composition of water in Lake Alchichica results from mixing two groundwater flow paths.

Considering that water circulates through the same geological materials but with different chemical compositions in SE and SW, it is inferred that groundwater evolves in two distinct flow paths influenced by faults. These faults, including La Preciosa, Piritas, La Ucha II, La Plateada I, and Las Pozas, come into contact with deeper rocks, triggering water–rock interactions with volcanic and carbonate formations, ultimately changing groundwater chemistry.

The two identified flow zones contribute differently to Lake Alchichica. The SE–NW direction represents a water–rock interaction process, increasing ionic concentration by weathering rock-forming minerals. In contrast, the SW–NE direction exhibits more evolved

water, with higher concentrations that decrease upon reaching the lake due to precipitation, particularly in Ca^{2+}, Mg^{2+}, Cl^{-}, and $HCO_3{}^{-}$.

The evolution of ions, particularly $HCO_3{}^{-}$, supports the presence of two distinct flow paths. Geochemical modeling elucidates that the dissolution of carbonate (calcite and dolomite) and silicate minerals (albite, amphibole, and kaolinite) is the source of $HCO_3{}^{-}$. This understanding aids in comprehending groundwater flow paths and their influence on crater lake hydrodynamics.

The geochemical evolution of groundwater's key processes are the precipitation of calcite, SiO_2(aq), and kaolinite, and the dissolution of CO_2(g), H_2O, and albite. Meanwhile, minerals such as gypsum, dolomite, and halite are in dissolution and precipitation; and plagioclase, amphibole, and biotite are in dissolution. They are conditioned on the location of the flow path or, to be more precise, the flow direction.

In summary, groundwater geochemical evolution involves the precipitation and dissolution of various minerals, with distinct water–rock interaction processes in the identified flow paths. The groundwater undergoes further changes as it traverses Lake Alchichica, resulting in a new composition and a mixture of evolved groundwater and lake water, as exemplified by the highest $HCO_3{}^{-}$ values in sample 44. This insight is crucial for comprehending the conditions leading to the formation of the stromatolite ring through the interchange of these water masses.

The decline in water levels is not associated with the identified water–rock interaction processes, as Lake Alchichica experiences evaporation, while the sampled groundwater sites do not. A comprehensive basin-wide investigation, which encompasses other maar lakes and their respective water–rock interaction processes, is imperative. Additionally, it is crucial to factor in the impact of intensive groundwater extraction on the observed decrease in water levels. This decline poses a threat to the survival of stromatolites.

The study emphasizes the complex processes influencing groundwater-feeding maar lakes and underscores the significance of understanding their geochemical origin and behavior for effective preservation and management.

The application of geochemical models is proposed for further global research of maar lakes, as it is expected this will contribute to a deeper understanding of their hydrochemistry and unique characteristics that foster endemicity.

Author Contributions: Conceptualization, S.O.-O., J.A., O.E. and R.A.S.-A.; methodology, S.O.-O., R.A.S.-A., J.R.F.-P., K.A.A.-F. and L.A.O.; software, S.O.-O.; validation, S.O.-O., E.M.-C. and J.A.; formal analysis, S.O.-O. and R.A.S.-A.; investigation, S.O.-O., O.E., J.A. and E.M.-C.; resources, J.A. and O.E.; data curation, S.O.-O. and R.A.S.-A.; writing—original draft preparation, S.O.-O. and R.A.S.-A.; writing—review and editing, S.O.-O., J.A., O.E., E.M.-C. and R.A.S.-A.; visualization, S.O.-O.; supervision, J.A. and E.M.-C.; project administration, J.A. and O.E.; funding acquisition, J.A. and O.E. All authors have read and agreed to the published version of the manuscript.

Funding: This research was funded by the Universidad Nacional Autónoma de México DGAPA/PAPIIT through the projects IN219220 and IN213323.

Data Availability Statement: The data presented in this study are available on request from the corresponding author (accurately indicate status).

Acknowledgments: We would like to thank the Dirección General de Asuntos del Personal, Universidad Nacional Autónoma de México for the postdoctoral grants awarded to Olea-Olea, S.R.S.A. would also like to thank CONACYT for doctoral scholarship 82851.

Conflicts of Interest: The authors declare no conflict of interest.

References

1. Li, M.; Li, C.; Xie, L.; Huang, W.; Zheng, Q.; Tan, K.; Hong, Y. Astronomical Tide and Storm Surge Signals Observed in an Isolated Inland Maar Lake Near the Coast. *J. Mar. Sci. Eng.* **2021**, *9*, 485. [CrossRef]
2. Hutchinson, G.E. *A Treatise on Limnology, Vol I, Part 1—Geography and Physics of Lakes*; Wiley: New York, NY, USA, 1957; ISBN 0-471-42568-0.
3. Jones, I.D.; Smol, J.P. Wetzel's Limnology. In *Lakes and River Ecosystems*; Academic Press: London, UK, 2024; ISBN 978-0-12-822701-5.

4. Williamson, C.E.; Dodds, W.; Kratz, T.K.; Palmer, M.A. Lakes and Streams as Sentinels of Environmental Change in Terrestrial and Atmospheric Processes. *Front. Ecol. Environ.* **2008**, *6*, 247–254. [CrossRef]
5. Aguilar, J.I.; Mendoza-Pascual, M.U.; Padilla, K.S.A.R.; Papa, R.D.S.; Okuda, N. Mixing Regimes in a Cluster of Seven Maar Lakes in Tropical Monsoon Asia. *Inl. Waters* **2023**, *13*, 47–61. [CrossRef]
6. Guoqiang, C.; Jiaqi, L. Maar Lakes in China and Their Significance in Paleoclimatic Research. *Acta Petrol. Sin.* **2018**, *31*, 4–12.
7. Jia, G.; Bai, Y.; Yang, X.; Xie, L.; Wei, G.; Ouyang, T.; Chu, G.; Liu, Z.; Peng, P. Biogeochemical Evidence of Holocene East Asian Summer and Winter Monsoon Variability from a Tropical Maar Lake in Southern China. *Quat. Sci. Rev.* **2015**, *111*, 51–61. [CrossRef]
8. Wang, W.; Liu, J.; Liu, D.; Liu, T.; Peng, P.; Lu, H.; Gu, Z.; Chu, G.; Negendank, J.; Luo, X.; et al. The Two-Step Monsoon Changes of the Last Deglaciation Recorded in Tropical Maar Lake Huguangyan, Southern China. *Chin. Sci. Bull.* **2000**, *45*, 1529–1532. [CrossRef]
9. Williamson, D.; Jelinowska, A.; Kissel, C.; Tucholka, P.; Gibert, E.; Gasse, F.; Massault, M.; Taieb, M.; Van Campo, E.; Wieckowski, K. Mineral-Magnetic Proxies of Erosion/Oxidation Cycles in Tropical Maar-Lake Sediments (Lake Tritrivakely, Madagascar): Paleoenvironmental Implications. *Earth Planet. Sci. Lett.* **1998**, *155*, 205–219. [CrossRef]
10. Williamson, D.; Jackson, M.J.; Banerjee, S.K.; Marvin, J.; Merdaci, O.; Thouveny, N.; Decobert, M.; Gibert-Massault, E.; Massault, M.; Mazaudier, D.; et al. Magnetic Signatures of Hydrological Change in a Tropical Maar-Lake (Lake Massoko, Tanzania): Preliminary Results. *Phys. Chem. Earth Part A Solid Earth Geod.* **1999**, *24*, 799–803. [CrossRef]
11. Garcin, Y.; Williamson, D.; Taieb, M.; Vincens, A.; Mathé, P.-E.; Majule, A. Centennial to Millennial Changes in Maar-Lake Deposition during the Last 45,000 Years in Tropical Southern Africa (Lake Masoko, Tanzania). *Palaeogeogr. Palaeoclimatol. Palaeoecol.* **2006**, *239*, 334–354. [CrossRef]
12. Alcocer, J. (Ed.) *Lago Alchichica: Una Joya de Biodiversidad*; Facultad de Estudios Superiores Iztacala, Universidad Nacional Autónoma de México; Comisión Nacional para el Conocimiento y Uso de la Biodiversidad: Mexico State, Mexico, 2019; ISBN 978-607-30-2278-1.
13. Alcocer, J. (Ed.) *Lake Alchichica Limnology*; Springer International Publishing: Cham, Switzerland, 2022; ISBN 978-3-030-79095-0.
14. Kaźmierczak, J.; Kempe, S.; Kremer, B.; López-García, P.; Moreira, D.; Tavera, R. Hydrochemistry and Microbialites of the Alkaline Crater Lake Alchichica, Mexico. *Facies* **2011**, *57*, 543–570. [CrossRef]
15. Arriaga-Cabrera, L.; Aguilar-Sierra, V.; Alcocer-Durán, J.; Jiménez-Rosenberg, R.; Muñoz-López, E.; Vázquez-Domínguez, E. *Regiones Hidrológicas Prioritarias: Fichas Técnicas y Mapa (Escala 1:4,000,000)*; Comisión Nacional Para El Conocimiento y Uso de La Biodiversidad: Mexico City, Mexico, 1998.
16. Appelo, C.A.J.; Postma, D. *Geochemistry, Groundwater and Pollution*, 2nd ed.; Balkema, P.A.A., Ed.; CRC Press: Boca Raton, FL, USA, 2005.
17. Parkhurst, D.L.; Appelo, C.A.J. User's Guide to Phreeqc (Version 2)—A Computer Program for Speciation, Batch Reaction, One Dimensional Transport, and Inverse Geochemical Calculations. *Water-Resour. Investig. Rep.* **1999**, *99*, 312.
18. Plummer, L. Geochemical Modeling of Water-Rock Interaction: Past, Present, Future. In Proceedings of the Seventh International Symposium on Water-Rock Interaction, Park City, UT, USA, 13–18 July 1992; Kharaka, Y.K., Ed.; Amsterdam, The Netherlands, 1992; pp. 23–33. Available online: https://www.academia.edu/24612511/Geochemical_modelling_of_water_rock_interaction (accessed on 23 February 2024).
19. Alcocer, J.; Lewis, W.M.; Hernández, M.D.C.; Oseguera, L.A.; Pérez, V.J.J.; Prat, N. Habitat Expansion of a Tropical Chironomid by Seasonal Alternation in Use of Littoral and Profundal Zones. *J. Limnol.* **2022**, *81*, 1–10. [CrossRef]
20. Escobar-Briones, E.; Alcocer, J. Caecidotea Williamsi (Crustacea: Isopoda: Asellidae), a New Species from a Saline Crater-Lake in the Eastern Mexican Plateau. *Hydrobiologia* **2002**, *477*, 93–105. [CrossRef]
21. Oliva, M.G.; Lugo, A.; Alcocer, J.; Peralta, L.; Sánchez, M.R. Alcocer Phytoplankton Dynamics in a Deep, Tropical, Hyposaline Lake. *Hydrobiologia* **2001**, *466*, 299–306. [CrossRef]
22. Ortega-Mayagoitia, E.; Vilaclara, G.; Alcántara-Hernández, R.J.; Macek, M. Diversity and Endemisms. In *Lake Alchichica Limnology*; Springer International Publishing: Cham, Switzerland, 2022; pp. 331–353.
23. Hernández, M.D.C.; Alcocer, J.; Oseguera, L.A.; Escobar, E. Profundal Benthic Invertebrates in an Oligotrophic Tropical Lake: Different Strategies for Coping with Anoxia. *J. Limnol.* **2014**, *2*, 387–399. [CrossRef]
24. Ardiles, V.; Alcocer, J.; Vilaclara, G.; Oseguera, L.A.; Velasco, L. Diatom Fluxes in a Tropical, Oligotrophic Lake Dominated by Large-Sized Phytoplankton. *Hydrobiologia* **2012**, *679*, 77–90. [CrossRef]
25. Alcocer, J.; Escobar, E.; Lugo, A. Littoral Benthos of the Saline Crater Lakes of the Basin of Oriental, Mexico. *Int. J. Salt Lake Res.* **1998**, *7*, 87–108. [CrossRef]
26. Alcocer, J.; Lugo, A.; Escobar, E.; Sànchez, M.R.; Vilaclara, G. Water Column Stratification and Its Implications in the Tropical Warm Monomictic Lake Alchichica, Puebla, Mexico. *Int. Ver. Für Theor. Und Angew. Limnol. Verhandlungen* **2000**, *27*, 3166–3169. [CrossRef]
27. Alcocer, J.; Lugo, A.; Fernández, R.; Vilaclara, G.; Oliva, M.G.; Oseguera, L.A.; Silva-Aguilera, R.A.; Escolero, Ó. 20 Years of Global Change on the Limnology and Plankton of a Tropical, High-Altitude Lake. *Diversity* **2022**, *14*, 190. [CrossRef]
28. Filonov, A.; Tereshchenko, I.; Alcocer, J.; Monzón, C. Dynamics of Internal Waves Generated by Mountain Breeze in Alchichica Crater Lake, Mexico. *Geofísica Int.* **2015**, *54*, 21–30. [CrossRef]
29. Oseguera, L.A.; Alcocer, J.; Escobar, E. Seston Flux in a Tropical Saline Lake. *Int. Ver. Für Theor. Und Angew. Limnol. Verhandlungen* **2010**, *30*, 1477–1481. [CrossRef]

30. Salas de León, D.A.; Alcocer, J.; Ardiles Gloria, V.; Quiroz-Martínez, B. Estimation of the Eddy Diffusivity Coefficient in a Warm Monomictic Tropical Lake. *J. Limnol.* **2016**, *75*, 161–168. [CrossRef]
31. Silva-Aguilera, R.A.; Vilaclara, G.; Armienta, M.A.; Escolero, Ó. Hydrogeology and Hydrochemistry of the Serdán-Oriental Basin and the Lake Alchichica. In *Lake Alchichica Limnology*; Springer International Publishing: Cham, Switzerland, 2022; pp. 63–74.
32. Vilaclara, G.; Chávez, M.; Lugo, A.; González, H.; Gaytán, M. Comparative Description of Crater-Lakes Basic Chemistry in Puebla State, Mexico. *Int. Ver. Für Theor. Und Angew. Limnol. Verhandlungen* **1993**, *25*, 435–440. [CrossRef]
33. Armienta, M.A.; Vilaclara, G.; De la Cruz-Reyna, S.; Ramos, S.; Ceniceros, N.; Cruz, O.; Aguayo, A.; Arcega-Cabrera, F. Water Chemistry of Lakes Related to Active and Inactive Mexican Volcanoes. *J. Volcanol. Geotherm. Res.* **2008**, *178*, 249–258. [CrossRef]
34. Sigala, I.; Caballero, M.; Correa-Metrio, A.; Lozano-García, S.; Vázquez, G.; Pérez, L.; Zawisza, E. Basic Limnology of 30 Continental Waterbodies of the Transmexican Volcanic Belt across Climatic and Environmental Gradients. *Boletín la Soc. Geológica Mex.* **2017**, *69*, 313–370. [CrossRef]
35. Mancilla Villa, O.R.; Bautista Olivas, A.L.; Ortega Escobar, H.M.; Sánchez Bernal, E.I.; Can Chulim, Á.; Guevara Gutiérrez, R.D.; Ortega Mikolaev, Y.M. Hidrogeoquímica de Salinas Zapotitlán y Los Lagos-Cráter Alchichica y Atexcac, Puebla. *Idesia (Arica)* **2014**, *32*, 55–69. [CrossRef]
36. Kouassi, A.M.; Ahoussi, K.E.; Kouakou, K.E.; Mamadou, A.; Biemi, J. Analyse Comparative Entre La Distribution Des Fréquences de Conductivité Électrique et Les Faciès Géochimiques Des Eaux Des Aquifères de Socle (Côte d'Ivoire). *Int. J. Biol. Chem. Sci.* **2016**, *10*, 435. [CrossRef]
37. Thomas, J.M.; Welch, A.H.; Preissler, A.M. Geochemical Evolution of Ground Water in Smith Creek Valley—A Hydrologically Closed Basin in Central Nevada, U.S.A. *Appl. Geochem.* **1989**, *4*, 493–510. [CrossRef]
38. Güler, C.; Thyne, G.D. Hydrologic and Geologic Factors Controlling Surface and Groundwater Chemistry in Indian Wells-Owens Valley Area, Southeastern California, USA. *J. Hydrol.* **2004**, *285*, 177–198. [CrossRef]
39. Demirel, Z.; Güler, C. Hydrogeochemical Evolution of Groundwater in a Mediterranean Coastal Aquifer, Mersin-Erdemli Basin (Turkey). *Environ. Geol.* **2006**, *49*, 477–487. [CrossRef]
40. Gastmans, D.; Hutcheon, I.; Menegário, A.A.; Chang, H.K. Geochemical Evolution of Groundwater in a Basaltic Aquifer Based on Chemical and Stable Isotopic Data: Case Study from the Northeastern Portion of Serra Geral Aquifer, São Paulo State (Brazil). *J. Hydrol.* **2016**, *535*, 598–611. [CrossRef]
41. Mahlknecht, J.; Steinich, B.; Navarro De León, I. Groundwater Chemistry and Mass Transfers in the Independence Aquifer, Central Mexico, by Using Multivariate Statistics and Mass-Balance Models. *Environ. Geol.* **2004**, *45*, 781–795. [CrossRef]
42. Mahlknecht, J.; Gárfias-Solis, J.; Aravena, R.; Tesch, R. Geochemical and Isotopic Investigations on Groundwater Residence Time and Flow in the Independence Basin, Mexico. *J. Hydrol.* **2006**, *324*, 283–300. [CrossRef]
43. Morán-Ramírez, J.; Ledesma-Ruiz, R.; Mahlknecht, J.; Ramos-Leal, J.A. Rock-Water Interactions and Pollution Processes in the Volcanic Aquifer System of Guadalajara, Mexico, Using Inverse Geochemical Modeling. *Appl. Geochem.* **2016**, *68*, 79–94. [CrossRef]
44. Olea-Olea, S.; Escolero, O.; Mahlknecht, J.; Ortega, L.; Taran, Y.; Moran-Zenteno, D.J.; Zamora-Martinez, O.; Tadeo-Leon, J. Water-Rock Interaction and Mixing Processes of Complex Urban Groundwater Flow System Subject to Intensive Exploitation: The Case of Mexico City. *J. S. Am. Earth Sci.* **2020**, *103*, 102719. [CrossRef]
45. Olea-Olea, S.; Escolero, O.; Mahlknecht, J.; Mona, J.; Ortega, L.; Beramendi-Orosco, L.; Zamora-Martinez, O.; Tadeo-Leon, J. Understanding the Processes in a Historically Relevant Thermal and Mineral Spring Water by Using Mixing and Inverse Geochemical Models. *Environ. Geochem. Health* **2022**, *44*, 2301–2323. [CrossRef] [PubMed]
46. SMN Station-21052. Available online: https://smn.conagua.gob.mx/es/ (accessed on 19 August 2023).
47. Alcocer, J.; Escolero, O.; Marín, L. Problemática Del Agua de La Cuenca Oriental, Estados de Puebla, Veracruz y Tlaxcala. In *El Agua en Mexico Vista Desde la Academia*; Blanca, J., Marin, L., Eds.; Academia Mexicana de Ciencias: Mexico City, México, 2004; pp. 57–77.
48. Can, Á.; Ortega, H.; García, N.; Reyes, A.; González, V.; Flores, D. Origen y Calidad Del Agua Subterránea En La Cuenca Oriental de México. *Terra Latinoam* **2011**, *29*, 189–200.
49. SOAPAP (Sistema Operador de los Servicios de Agua Potable y Alcantarillado de Puebla). *Estudio de Las Fuentes de Abastecimiento Para El Suministro de Agua Potable Para El Programa de Desarrollo Regional Angelópolis*; de C.V., S.A., Ed.; Grupo de Ingeniería En Consultorías y Obras: Puebla, Mexico, 1997.
50. Alcala, A. Estudio Hidrogeológico de Alchichica, Estado de Puebla. Bachelor Thesis, Universidad Nacional Autonóma de México, México, 2004. Available online: http://132.248.9.195/ppt2004/0335824/Index.html (accessed on 10 September 2023).
51. Garcia, J. Efectos Climáticos Sobre El Agua Subterránea y El Lago Alchichica Puebla, México. Master's Thesis, Universidad Nacional Autonóma de México, México, 2010. Available online: http://132.248.9.195/ptb2010/octubre/0663329/Index.html (accessed on 16 August 2023).
52. Menesses, L. Exploración Geofísica e Hidrogeológica En La Laguna de Alchichica, Cuenca de Libres-Oriental, Estado de Puebla, UNAM. Bachelor Thesis, Universidad Nacional Autonóma de México, México, 2002. Available online: http://132.248.9.195/ppt2002/0312163/Index.html (accessed on 22 September 2023).
53. Silva-Aguilera, R. Análisis Del Descenso Del Nivel Del Agua En El Lago de Alchichica, Puebla. Master Thesis, Universidad Nacional Autonóma de México, México, 2019. Available online: http://132.248.9.195/ptd2019/junio/0789822/Index.html (accessed on 30 July 2023).

54. SGM Carta Geológica Guadalupe Victoria E14-B35 1998. Available online: http://Mapserver.sgm.gob.mx/Cartas_Online/geologia/1891_E14-B35_GM.pdf (accessed on 11 August 2023).
55. Chako-Tchamabé, B.; Carrasco-Núñez, G.; Miggins, D.P.; Németh, K. Late Pleistocene to Holocene Activity of Alchichica Maar Volcano, Eastern Trans-Mexican Volcanic Belt. *J. S. Am. Earth Sci.* **2020**, *97*, 102404. [CrossRef]
56. Carrasco-Núñez, G.; Ort, M.H.; Romero, C. Evolution and Hydrological Conditions of a Maar Volcano (Atexcac Crater, Eastern Mexico). *J. Volcanol. Geotherm. Res.* **2007**, *159*, 179–197. [CrossRef]
57. Gasca, A. Algunas Notas de La Génesis de Los Lagos-Cráter de La Cuenca de Oriental. Puebla-Tlaxcala-Veracruz. *Inst. Nac. Antropol. e Hist. Colección Científica Prehist.* **1981**, *98*, 55.
58. Chako-Tchamabé, B.; Carrasco-Núñez, G.; Gountié Dedzo, M.; Kshirsagar, P.; Asaah, A.N.E. Geochemical Characterization of Alchichica Maar Volcano, Serdán-Oriental Basin, Eastern Trans-Mexican Volcanic Belt: Insights on Polymagmatic Evolution at Monogenetic Volcanic Clusters. *J. S. Am. Earth Sci.* **2020**, *104*, 102889. [CrossRef]
59. *EPA METHOD 200.7—Determination of Elements and Trace Elements in Water and Wastes by Inductively Coupled Plasma-Atomic Emmission Spectropemtry*; Agency, U.E.P., Ed.; Washington, DC, USA. 1994; Volume 600. Available online: https://www.epa.gov/sites/default/files/2015-06/documents/epa-200.7.pdf (accessed on 6 December 2023).
60. EPA6010D Inductively Coupled Plasma—Optical Emission Spectrometry 2014. Available online: https://www.epa.gov/sites/default/files/2015-12/documents/6010d.pdf (accessed on 6 December 2023).
61. Freeze, R.A.; Cherry, J. Groundwater. Prentice-Hall, Ed.; Prentice-Hall, Inc.: Englewood Cliffs, NJ, USA, 1979; ISBN 0133653129.
62. Cressie, N. *Statistics for Spatial Data*; John Wiley & Sons: New York, NY, USA, 1993.
63. Franke, R. Scattered Data Interpolation: Tests of Some Methods. *Math. Comput.* **1982**, *38*, 181. [CrossRef]
64. Piper, A.M. A Graphic Procedure in the Geochemical Interpretation of Water Analyses. *Trans. Am. Geophys. Union* **1944**, *25*, 914–924.
65. Gibbs, R.J. Mechanisms Controlling World Water Chemistry. *Science* **1970**, *170*, 1081–1090. [CrossRef]
66. Marandi, A.; Shand, P. Groundwater Chemistry and the Gibbs Diagram. *Appl. Geochem.* **2018**, *97*, 209–212. [CrossRef]
67. Garrels, R.M.; Charles, C. *Solutions, Minerals, and Equilibria*, 1st ed.; Jones and Bartlett: Boston, MA, USA, 1965.
68. Galeczka, I.; Wolff-Boenisch, D.; Oelkers, E.H.; Gislason, S.R. An Experimental Study of Basaltic Glass–H_2O–CO_2 Interaction at 22 and 50 °C: Implications for Subsurface Storage of CO_2. *Geochim. Cosmochim. Acta* **2014**, *126*, 123–145. [CrossRef]
69. Université d'Ottawa, C. Chapter 5 Geochemical Weathering. Available online: https://mysite.science.uottawa.ca/idclark/GEO4342/2009/Weathering.pdf (accessed on 16 September 2023).
70. Walraevens, K.; Bakundukize, C.; Mtoni, Y.E.; Van Camp, M. Understanding the Hydrogeochemical Evolution of Groundwater in Precambrian Basement Aquifers: A Case Study of Bugesera Region in Burundi. *J. Geochemical Explor.* **2018**, *188*, 24–42. [CrossRef]
71. Parkhurst, D.L.; Plummer, L.N.; Thorstenson, D.C. *BALANCE-A Computer Program for Geochemical Calculations*; U. S. Geological Survey Water Resources. Inv. Rep. USA: Boston, VA, USA, 1982.
72. Plummer, L.N. Geochemical Modeling: A Comparison of Forward and Inverse Methods. In Proceedings of the First Canadian/American Conference on Hydrogeology: Practical Applications of Ground Water Geochemistry, Banff, AB, Canada, 22–26 June 1984; National Water Well Association: Red Deer, AB, Canada, 1984; pp. 149–177.
73. Plummer, L.N.; Parkhurst, D.L.; Thorstenson, D.C. Devel-Opment of Reaction Models for Ground-Water Systems. *Geochim. Cosmochim. Acta* **1983**, *47*, 665–686. [CrossRef]
74. Parkhurst, D.L.; Thorstenson, D.C.; Plummer, L.N. *PHREEQE, a Computer Program for Geochemical Calculations*; U. S. Geological Survey Water Resources. Inv. Rep. USA: Boston, VA, USA, 1980.
75. Zhu, C.; Anderson, G. *Environmental Applications of Geochemical Modeling*, 1st ed.; Press, C.U., Ed.; Cambridge University Press: Cambridge, UK, 2002; ISBN 9780521809078.
76. Taylor, E.H. A New Ambystomid Salamander Adapted to Brackish Water. *Copeia* **1943**, *1943*, 151. [CrossRef]
77. Parkhurst, D.L.; Appelo, C.A.J. Description of Input and Examples for PHREEQC Version 3—A Computer Program for Speciation, Batch-Reaction, One-Dimensional Transport, and Inverse Geochemical Calculations. *US Geol. Surv. Tech. Methods* **2013**, *6*, 504.
78. Xu, P.; Qian, H.; Li, S.; Li, W.; Chen, J.; Liu, Y. Geochemical Evidence of Fluoride Behavior in Loess and Its Influence on Seepage Characteristics: An Experimental Study. *Sci. Total Environ.* **2023**, *882*, 163564. [CrossRef] [PubMed]
79. Li, X.; Huang, X.; Liao, X.; Zhang, Y. Hydrogeochemical Characteristics and Conceptual Model of the Geothermal Waters in the Xianshuihe Fault Zone, Southwestern China. *Int. J. Environ. Res. Public Health* **2020**, *17*, 500. [CrossRef]
80. Berkani, C.; Boulabeiz, M.; Dali, N.; Sedrati, A.; Houh, B. Hydrogeochemical modeling of groundwater of the quaternary aquifer in Mellagou valley -Bouhmama- (northeastern Algeria). *Carpathian J. Earth Environ. Sci.* **2023**, *18*, 115–126. [CrossRef]
81. Escario, S.; Seigneur, N.; Collet, A.; Regnault, O.; de Boissezon, H.; Lagneau, V.; Descostes, M. A Reactive Transport Model Designed to Predict the Environmental Footprint of an 'in-Situ Recovery' Uranium Exploitation. *J. Contam. Hydrol.* **2023**, *254*, 104106. [CrossRef]
82. Zhang, X.; Ling, S.; Wu, X.; Wang, F.; Wang, J.; Teng, Q.; Xie, J. Hydrochemistry Process and Microweathering Behaviour of Sandstone Heritages in the Nankan Grotto, China: Insights from Field Micro-Observations and Water–Rock Interaction Experiments. *Bull. Eng. Geol. Environ.* **2023**, *82*, 356. [CrossRef]
83. Sajil Kumar, P.J.; Jegathambal, P.; Nair, S.; James, E.J. Temperature and PH Dependent Geochemical Modeling of Fluoride Mobilization in the Groundwater of a Crystalline Aquifer in Southern India. *J. Geochem. Explor.* **2015**, *156*, 1–9. [CrossRef]

84. Zhao, X.; Xu, Z.; Sun, Y. Mechanism of Changes in Goaf Water Hydrogeochemistry: A Case Study of the Menkeqing Coal Mine. *Int. J. Environ. Res. Public Health* **2022**, *20*, 536. [CrossRef]
85. Demer, S.; Elitok, Ö.; Memiş, Ü. Origin and Geochemical Evolution of Groundwaters at the Northeastern Extend of the Active Fethiye-Burdur Fault Zone within the Ophiolitic Teke Nappes, SW Turkey. *Arab. J. Geosci.* **2019**, *12*, 783. [CrossRef]
86. Lucas, Y.; Chabaux, F.; Clément, A.; Fritz, B.; Ranchoux, C.; Ackerer, J.; Pelt, E.; Schmitt, A.-D.; Stille, P. Hydrogeochemical Modeling of the Spatiotemporal Variations in 87Sr/86Sr Isotope Ratios and Sr Concentrations of Spring Waters in a Headwater Catchment (Strengbach CZO–France). *Chem. Geol.* **2023**, *616*, 121216. [CrossRef]
87. Helms, T.S.; McSween, H.Y.; Labotka, T.C.; Jarosewich, E. Petrology of a Georgia Blue Ridge Amphibolite Unit with Hornblende + Gedrite + Kyanite + Staurolite. *Am. Mineral.* **1987**, *11*, 1086–1096.
88. Teramoto, E.H.; Stradioto, M.R.; Chang, H.K. Geochemical Simulation to Assess the Rock–Water Interaction in Crystalline Aquifers in São Paulo State, Southeastern Brazil. *Sustain. Water Resour. Manag.* **2023**, *9*, 162. [CrossRef]
89. Gómez, P.; Turrero, M.P.J. Una Revision de Los Procesos Geoquímicos de Baja Temperatura En La Interacción Agua-Roca. *Estud. Geológicos* **1994**, *50*, 345–357.
90. Garrels, R.M. Genesis of Some Ground Waters from Igneous Rocks. *Res. Geochem.* **1967**, *2*, 405–420.
91. Hanley, J.J.; Mungall, J.E. Chlorine Enrichment and Hydrous Alteration of the Sudbury Breccia Hosting Footwall Cu-Ni-PGE Mineralization at the Fraser Mine, Sudbury, Ontario, Canada. *Can. Mineral.* **2003**, *41*, 857–881. [CrossRef]
92. Léger, A.; Rebbert, C.; Webster, J. Cl-Rich Biotite and Amphibole from Black Rock Forest, Cornwall, New York. *Am. Mineral.* **1996**, *81*, 495–504. [CrossRef]
93. Volfinger, M.; Robert, J.L.; Vielzeuf, D.; Neiva, A.M.R. Structural Control of the Chlorine Content of OH-Bearing Silicates (Micas and Amphiboles). *Geochim. Cosmochim.* **1985**, *49*, 37–48. [CrossRef]